Respiratory Physiology & Neurobiology 177 (2011) 141–148

View metadata, citation and similar papers at core.ac.uk

brought to you by CORE

provided by Elsevier - Publisher Connector

Respiratory Physiology & Neurobiology

journal homepage: www.elsevier.com/locate/resphysiol

Impact of obesity on airway and lung parenchyma remodeling in experimental chronic allergic asthma

Simone A. Saraiva[a], Adriana L. Silva[a], Débora G. Xisto[a], Soraia C. Abreu[a], Johnatas D. Silva[a], Pedro L. Silva[a], Tatiana P.F. Teixeira[b], Edwin R. Parra[c], Ana Laura N. Carvalho[c], Raquel Annoni[c], Thais Mauad[c], Vera L. Capelozzi[c], Patricia M.R. Silva[b], Marco A. Martins[b], Patricia R.M. Rocco[a,*]

[a] *Laboratory of Pulmonary Investigation, Carlos Chagas Filho Biophysics Institute, Federal University of Rio de Janeiro, Rio de Janeiro, Brazil*
[b] *Laboratory of Inflammation, Oswaldo Cruz Institute, FIOCRUZ, Rio de Janeiro, Brazil*
[c] *Department of Pathology, University of São Paulo, São Paulo, Brazil*

ARTICLE INFO

Article history:
Accepted 22 March 2011

Keywords:
Airway
Asthma
Collagen fiber
Eosinophil
Electron microscopy

ABSTRACT

The impact of obesity on the inflammatory process has been described in asthma, however little is known about the influence of diet-induced obesity on lung remodeling. For this purpose, 56 recently weaned A/J mice were randomly divided into 2 groups. In the C group, mice were fed a standard chow diet, while OB animals received isocaloric high-fat diet to reach 1.5 of the mean body weight of C. After 12 weeks, each group was further randomized to be sensitized and challenged with ovalbumin (OVA) or saline. Twenty-four hours after the last challenge, collagen fiber content in airways and lung parenchyma, the volume proportion of smooth muscle-specific actin in alveolar ducts and terminal bronchiole, and the number of eosinophils in bronchoalveolar lavage fluid were higher in OB-OVA than C-OVA. In conclusion, diet-induced obesity enhanced lung remodeling resulting in higher airway responsiveness in the present experimental chronic allergic asthma.

© 2011 Elsevier B.V. Open access under the Elsevier OA license.

1. Introduction

Obesity has recently been identified as a major risk factor for the development of asthma. Asthma tends to be more severe in obese individuals, and it does not respond adequately to treatment. As a result, the combination of obesity and asthma is becoming a major public health issue in many countries (Dixon et al., 2010).

Asthma is a complex syndrome, characterized by inflammation of the airways associated with airway hyperresponsiveness and mucus hypersecretion (Bateman et al., 2008), and also often with lung remodeling (Elias et al., 1999; Davies et al., 2003). Experimental and clinical studies have demonstrated the potential effects of obesity on airway inflammation (Shore et al., 2003; Shore et al., 2006; Misso et al., 2008; Calixto et al., 2010) and airway hyperresponsiveness (Shore and Fredberg, 2005; Johnston et al., 2007). However, so far, there have been few studies analyzing the impact of obesity on the remodeling process. In this line, Medoff and colleagues have reported that adiponectin deficiency enhanced allergic airway inflammation and led to an increase in pulmonary arterial muscularization and pulmonary hypertension in animals with allergic inflammation (Medoff et al., 2009). Additionally, adiponectin deficiency did not modulate airway fibrosis. Nevertheless, adiponectin mimics only one component of the obese state; thus, the role of obesity in airway and lung parenchyma remodeling in asthma needs further elucidation.

The aim of the present study was to investigate the effect of obesity on the remodeling process in asthma and the relationship of these ultrastructural changes with airway responsiveness and inflammation in an experimental model of chronic allergic asthma.

2. Materials and methods

This study was approved by the Ethics Committee of the Carlos Chagas Filho Institute of Biophysics, Health Sciences Centre, Federal University of Rio de Janeiro. All animals received humane care in compliance with the "Principles of Laboratory Animal Care" formulated by the National Society for Medical Research and the "Guide for the Care and Use of Laboratory Animals" prepared by the National Academy of Sciences, USA.

* Corresponding author at: Laboratory of Pulmonary Investigation, Carlos Chagas Filho Biophysics Institute, Federal University of Rio de Janeiro, Centro de Ciências da Saúde, Avenida Carlos Chagas Filho, s/n, Bloco G-014, Ilha do Fundão 21941-902, Rio de Janeiro, RJ, Brazil. Tel.: +55 21 2562 6530; fax: +55 21 2280 8193.
E-mail addresses: prmrocco@biof.ufrj.br, prmrocco@gmail.com (P.R.M. Rocco).

1569-9048 © 2011 Elsevier B.V. Open access under the Elsevier OA license.
doi:10.1016/j.resp.2011.03.019

2.1. Animal preparation and experimental protocol

The experiments were performed in 56 newly weaned A/J male mice. Animals were maintained on a standard (C, 22% protein, 73% carbohydrate, 5% fat) or high-fat diet (OB, 12% protein, 52% carbohydrate, 36% fat). They received water *ad libitum* and were housed in micro-isolator cages (1/cage) with temperature control and a 12 h light:dark cycle. During 12 weeks, the body weight and food consumption of all mice were measured.

The animals were further randomized to be sensitized and challenged with sterile ovalbumin (Albumin from chicken egg white – A5503, Sigma–Aldrich®, St. Louis, MO, USA) or saline. In the chronic allergic asthma groups, mice were immunized by intraperitoneal injection of 10 μg sterile ovalbumin (OVA) in 0.1 ml saline on each of seven alternate days. Forty days after the beginning of sensitization, intratracheal challenge was performed with the following protocol: mice were treated with sevoflurane anesthesia. A 0.5-cm-long midline cervical incision was made to expose the trachea, and 20 μg OVA in 20 μl warm (37 °C) sterile saline (0.9% NaCl) were instilled. The cervical incision was closed with 5.0 silk suture and the mice were returned to their cage. The animals recovered rapidly after surgery. This procedure was performed three times, with a 3-day interval between instillations. No adjuvants were used in the present protocol (Xisto et al., 2005). The control group (SAL) received saline instead of ovalbumin during both sensitization and challenge. Ventilatory variables and lung histology were analyzed in 28 mice ($n = 7$/group) while airway hyperresponsiveness, dynamic compliance, and the inflammatory process in bronchoalveolar lavage fluid (BALF) were evaluated in a second group of 28 animals ($n = 7$/group). The mice were anesthetized and euthanized by sectioning abdominal aorta and vena cava, yielding a massive hemorrhage that quickly killed the animals. Visceral adipose tissues were dissected from each animal according to defined anatomic landmarks, and weighed after mice were killed.

2.2. Ventilatory variables

Twenty-four hours after the last challenge, the animals were sedated (diazepam 1 mg ip), anaesthetized (thiopental sodium 20 mg/kg ip), and tracheotomized. A pneumotachograph (1.5 mm ID, length = 4.2 cm, distance between side ports = 2.1 cm) was connected to the tracheal cannula for the measurements of airflow. The pressure gradient across the pneumotachograph was determined by a differential pressure transducer (SCIREQ, SC-24, Montreal, Canada). Tidal volume was obtained by integration of the flow signal. During spontaneous breathing, durations of inspiration and expiration and the respiratory cycle time were measured from flow signal. Using these variables, we calculated respiratory frequency (f) and minute ventilation (V'_E).

2.3. Chest wall configuration

Chest wall circumferences at the third intercostal space, xiphoid, and crista iliaca levels were measured as previously described (Zin et al., 1989; Maranhão et al., 2000). The measurements were performed three times by the same investigator in each animal at functional residual capacity. Special care was taken to perform the measurements at the same reference points and to avoid errors due to the soft tissue compressibility.

2.4. Airway responsiveness

Airway responsiveness was assessed 24 h after the last challenge with aerosolized methacholine in a FinePoint R/C Buxco Platform (Buxco Electronics, Sharon, CT, USA). Mice were anaesthetized with nembutal (60 mg/kg). Neuromuscular activity was blocked with bromide pancuronium (1 mg/kg). Airflow and transpulmonary pressure were recorded using a Buxco Pulmonary Mechanics Processing System (Buxco Electronics, Wilmington, NC, USA). This instrument was used to calculate airway resistance and dynamic compliance (Cdyn). Analog signals from the computer were digitized using a Buxco analog to digital converter (Buxco Electronics). Mice were allowed to stabilize for 5 min and increasing concentrations of methacholine (3, 6 and 12 mg/mL) were aerosolized for 5 min each. Baseline resistance and Cdyn were assessed with aerosolized phosphate-buffered saline (PBS). The results were expressed as the mean absolute values of lung resistance and Cdyn responses recorded during 5 min after the administration of methacholine aerosol.

2.5. Lung histology

A laparotomy was performed immediately after determination of the ventilatory variables, and heparin (1000 IU) was intravenously injected in the vena cava. The trachea was clamped at end-expiration (PEEP = 2 cmH_2O), and the abdominal aorta and vena cava were sectioned, yielding a massive hemorrhage that quickly killed the animals. The right lung was then removed, fixed in 3% buffered formaldehyde and paraffin embedded. Four-μm-thick slices were cut and stained with hematoxylin–eosin.

Lung morphometry analysis was performed with an integrating eyepiece with a coherent system consisting of a grid with 100 points and 50 lines (known length) coupled to a conventional light microscope (Olympus BX51, Olympus Latin America-Inc., Brazil). Fraction areas of collapsed and normal lung were determined by the point-counting technique (Hsia et al., 2010) across 10 random, non-coincident microscopic fields (Menezes et al., 2005; Santos et al., 2006). Briefly, points falling on collapsed or normal pulmonary areas were counted and divided by the total number of points in each microscopic field.

Airway bronchoconstriction index was determined by counting the points falling on the airway lumen and those falling on airway smooth muscle and on the epithelium, at a magnification of 400×. The perimeter of the airways was estimated by counting the intercepts of the lines of the integrating eyepiece with the epithelial basal membrane. The areas of smooth muscle and airway epithelium were corrected in terms of airway perimeter by dividing their values by the number of intercepts of the line system with the epithelial basal membrane of the corresponding airway. Because the number of intercepts (NI) of the lines with the epithelial basal membrane is proportional to the airway perimeter, and the number of points (NP) falling on airway lumen is proportional to airway area, the magnitude of bronchoconstriction (contraction index, CI) was computed by the relationship $CI = NI/\sqrt{NP}$. Measurements were performed in five airways from each animal at 400× magnification (Silva et al., 2008; Antunes et al., 2010).

Collagen (Picrosirius-polarization method) (Montes, 1996) and elastic fibers (Weigert's resorcin fuchsin method with oxidation) (Fullmer et al., 1974) were quantified in the alveolar septa and airways. Alveolar septa quantification was carried out with the aid of a digital analysis system and specific software (Image-Pro® Plus 5.1 for Windows® Media Cybernetics – Silver Spring, MD, USA) under 200× magnification. The images were generated by a microscope (Axioplan, Zeiss, Oberkochen, Germany) connected to a camera (Sony Trinitron CCD, Sony, Tokyo, Japan), fed into a computer through a frame grabber (Oculus TCX, Coreco Inc., St Laurent, PQ, Canada) for off-line processing. The thresholds for collagen and elastic fibers were established after enhancement of contrast up to the point where the fiber was easily identified as either birefringent (collagen) or black (elastic) bands. Bronchi and blood vessels were carefully avoided during the measurements. The area occupied by fibers was determined by digital densitometric recognition.

To avoid any bias due to alveolar collapse, the areas occupied by elastic and collagen fibers in each alveolar septum were divided by the length of each studied septum. The results were expressed as the amount of elastic and collagen fibers per unit of septum length ($\mu m^2/\mu m$). Collagen and elastic fiber content was quantified in the whole circumference of the two largest, transversally cut airways present in the sections. Results were expressed as the area of collagen or elastic fibers divided by the perimeter of the basement membrane ($\mu m^2/\mu m$).

2.6. Immunohistochemistry

Right lungs were fixed in 4% paraformaldehyde and embedded in paraffin for immunohistochemistry using monoclonal antibody against α-smooth muscle actin (Dako, Carpenteria, CA, USA) at a 1:500 dilution. Sections were then rinsed with Tris-buffered saline and sequentially incubated with biotinylated rabbit antimouse IgG (Dako Corp., Cambridge, UK) at a dilution of 1:400, followed by streptavidin combined in vitro with biotinylated horseradish peroxidase at a dilution of 1:1000 (Dako, Cambridge, UK). The reaction product was developed using diaminobenzidine tetrahydrochloride. Sections were counterstained with hematoxylin for 1 min, dehydrated through graded alcohols, and mounted in resinous medium. Known positive controls were included with each run, and negative controls had the primary antibody omitted (Dolhnikoff et al., 1998). The analysis was performed on the slides stained for α-smooth muscle actin applying the point-counting technique (Weibel, 1990). Using a 121-point grid, we calculated the volume proportion of smooth-muscle-specific actin in terminal bronchioles and alveolar ducts as the relation between the number of points falling on actin-stained and non-stained tissue. Measurements were done at 400× magnification in each slide.

2.7. Transmission electron microscopy

Three 2 mm × 2 mm × 2 mm slices were cut from three different segments of the left lung and then fixed [2.5% glutaraldehyde and phosphate buffer 0.1 M (pH = 7.4)] for 60 min at −4 °C for electron microscopy (JEOL 1010 Transmission Electron Microscope, Tokyo, Japan). Ultrathin sections from selected areas were examined and micrographed in a JEOL electron microscope (JSM-6100F; Tokyo, Japan). Submicroscopic analysis of lung tissue showed that the extension and distribution of the parenchymal alterations were inhomogeneous along the bronchiole and alveolar tissue (alveolar ducts and alveoli). Thus, electron micrographs representative of the lung specimen (SAL and OVA groups) were enlarged to a convenient size to visualize the following inflammatory and remodeling structural defects in airways: (a) epithelial detachment, (b) eosinophil infiltration, (c) neutrophil infiltration, (d) degenerative changes of ciliated airway epithelial cells, (e) subepithelial fibrosis, (f) elastic fiber fragmentation, (g) smooth muscle hypertrophy, (h) myofibroblast hyperplasia, and (i) mucous cell hyperplasia (Jeffery et al., 1992; Antunes et al., 2010). Pathologic findings were graded according to a 5-point semi-quantitative severity-based scoring system as: 0 = normal lung parenchyma, 1 = changes in 1–25%, 2 = changes in 26–50%, 3 = changes in 51–75%, and 4 = changes in 76–100% of examined tissue. Fifteen electron microscopy images were analyzed per animal.

2.8. Evaluation of bronchoalveolar lavage fluid (BALF)

Lungs were lavaged via a tracheal tube with PBS solution (1 ml) containing EDTA (10 mN). Total leukocyte numbers were measured in Neubauer chambers under light microscopy after diluting the samples in Türk solution (2% acetic acid). Differential cell counts were performed in cytospin smears stained by the May-Grünwald-Giemsa method (Abreu et al., 2010; Antunes et al., 2010).

2.9. Statistical analysis

The normality of the data was tested using Kolmogorov-Smirnov's test with Lilliefors' correction, while Levene's median test was used to evaluate the homogeneity of variances. If both conditions were satisfied, two-way ANOVA followed by Tukey's test was used. To compare non-parametric data, two-way ANOVA on ranks followed by Dunn's post hoc test was selected. The significance level was set at 5%. Parametric data were expressed as mean ± SEM, while non-parametric data were expressed as median (interquartile range). All tests were performed using SigmaStat 3.1 (Jandel Corporation, San Raphael, CA, USA).

3. Results

Mean body and visceral adipose tissue weights were significantly increased after a 12 week high-fat diet compared with the standard diet, with no significant difference between SAL and OVA. Chest wall circumferences at the third intercostal space, xiphoid, and crista iliaca levels were higher in OB compared to C groups (Table 1). Tidal volume was lower in OB-SAL compared to C-SAL mice. High fat diet induced a reduction in f and V'_E in the SAL group. Conversely, both f and V'_E were higher in OB-OVA compared to OB-SAL group (Table 2).

The fraction area of alveolar collapse, bronchoconstriction index, collagen fiber content in airways and alveolar septa and the volume proportion of smooth-muscle-specific actin in terminal bronchioles and alveolar ducts (Table 3, Figs. 1 and 2) were higher in OVA compared to SAL. All these parameters were also increased in OB-SAL animals and further augmented in the OB-OVA group. Elastic fiber content in the airway and alveolar septa was similar in OVA and SAL animals receiving the standard diet, however, in OB mice the amount of elastic fiber was higher in the OVA than SAL group (Table 3).

Electron microscopy showed that the ingestion of a high fat diet yielded airway neutrophil infiltration and increased collagen fiber content. Airway epithelial cell detachment from the basement membrane was observed in OVA animals receiving the standard diet, along with degenerative changes in ciliated airway epithelial cells, eosinophil and neutrophil infiltration, myofibroblast and mucous cells hyperplasia, subepithelial fibrosis, smooth muscle hypertrophy, and elastic fiber fragmentation (Table 4, Fig. 3). However, the high fat diet led to a further increase in epithelial cell detachment, eosinophil and neutrophil infiltration, subepithelial fibrosis, elastic fiber fragmentation and mucous cell hyperplasia in OVA animals.

The total number of leukocytes, eosinophils, neutrophils, and mononuclear cells (Table 5) in BALF was higher in OVA compared to SAL in both C and OB groups, with a greater increase in OB.

The increase in airway resistance evoked by methacholine was significantly higher in the C-OVA than C-SAL group. OB-OVA exhibited a significant increase in airway resistance at methacholine doses of 6 and 12 mg/ml compared to OB-SAL. Cdyn was lower in C-OVA than C-SAL at methacholine doses of 6 and 12 mg/ml, and further reduced in OB-OVA independent of methacholine dose (Fig. 4).

4. Discussion

The present study found that diet-induced obesity enhanced airway and lung parenchyma remodeling, leading to greater airway hyperresponsiveness in a murine model of chronic allergic

Table 1
Initial and final body weight, visceral adipose tissue weight, and thoraco-abdominal circumference.

	C		OB	
	SAL	OVA	SAL	OVA
Initial body weight (g)	14.4 ± 3.1	14.3 ± 2.6	14.3 ± 1.2	14.2 ± 1.6
Final body weight (g)	21.5 ± 1.9	19.9 ± 1.8	29.7 ± 3.0[†]	32.4 ± 2.3[**]
Visceral adipose tissue weight (g)	0.4 ± 0.2	0.4 ± 0.1	3.5 ± 0.8[†]	3.4 ± 0.8[**]
Circumference at third intercostal space (cm)	6.0 ± 0.5	6.2 ± 0.6	6.9 ± 0.6[†]	6.9 ± 0.7[**]
Circumference at xiphoid (cm)	6.8 ± 0.5	6.9 ± 0.6	7.2 ± 0.8[†]	7.6 ± 0.6[**]
Circumference at crista iliaca (cm)	7.2 ± 0.4	7.2 ± 0.3	8.1 ± 0.9[†]	8.9 ± 1.0[**]

Values are mean ± SEM of 14 mice in each group. C: mice fed with a standard chow diet, OB: animals that received isocaloric high-fat diet. SAL: mice sensitized and challenged with saline, OVA: mice sensitized and challenged with ovalbumin.
[†] C-SAL *vs.* OB-SAL ($p < 0.05$).
[**] C-OVA *vs.* OB-OVA ($p < 0.05$).

Table 2
Ventilatory variables.

	C		OB	
	SAL	OVA	SAL	OVA
Tidal volume (ml)	0.16 ± 0.01	0.14 ± 0.01	0.11 ± 0.01[†]	0.12 ± 0.01
Respiratory frequency (bpm)	140 ± 15	158 ± 13	116 ± 8[†]	175 ± 20[**,#]
Minute ventilation (ml/min)	23.53 ± 4.07	22.21 ± 1.99	12.50 ± 1.24[†]	20.76 ± 2.92[#]

Values are mean ± SEM of 7 mice in each group. C: mice fed with a standard chow diet, OB: animals that received isocaloric high-fat diet. SAL: mice sensitized and challenged with saline, OVA: mice sensitized and challenged with ovalbumin.
[†] C-SAL *vs.* OB-SAL ($p < 0.05$).
[**] C-OVA *vs.* OB-OVA ($p < 0.05$).
[#] OB-SAL *vs.* OB-OVA ($p < 0.05$).

Table 3
Lung morphometry.

Groups		C		OB	
		SAL	OVA	SAL	OVA
Normal (%)		97.76 ± 0.32	90.75 ± 2.50[*]	87.73 ± 2.84[†]	75.67 ± 1.25[**,#]
Collapse (%)		2.27 ± 0.31	9.25 ± 2.50[*]	12.41 ± 2.78[†]	24.33 ± 1.25[**,#]
Airway bronchoconstriction index		1.86 ± 0.08	2.18 ± 0.12[*]	2.30 ± 0.14[†]	2.70 ± 0.16[**,#]
Collagen fiber ($\mu m^2/\mu m$)	Airways	2.47 ± .25	4.41 ± 0.50[*]	4.49 ± 0.38[†]	7.35 ± 0.98[**,#]
	Alveolar septa	0.045 ± 0.01	0.075 ± 0.01[*]	0.063 ± 0.01[†]	0.098 ± 0.01[**,#]
Elastic fiber ($\mu m^2/\mu m$)	Airways	1.89 ± 0.24	2.27 ± 0.22	1.99 ± 0.28	3.63 ± 0.48[**,#]
	Alveolar septa	0.34 ± 0.08	0.39 ± 0.10	0.35 ± 0.03	0.42 ± 0.04[#]
Actin (%)	Terminal bronchiole	7.3 ± 0.5	12.1 ± 0.4[*]	10.1 ± 0.6[†]	15.8 ± 0.5[**,#]
	Alveolar duct	5.4 ± 0.3	9.0 ± 0.4[*]	6.4 ± 0.5[†]	12.3 ± 0.7[**,#]

Values are mean ± SEM of 7 mice in each group. Fraction area of normal and collapsed alveoli, bronchoconstriction index, collagen and elastic fibers in airways and alveolar septa, and volume proportion of smooth-muscle specific actin in terminal bronchiole. C: mice fed with a standard chow diet, OB: animals that received isocaloric high-fat diet. SAL: mice sensitized and challenged with saline, OVA: mice sensitized and challenged with ovalbumin.
[*] C-SAL *vs.* C-OVA ($p < 0.05$).
[**] C-OVA *vs.* OB-OVA ($p < 0.05$).
[†] C-SAL *vs.* OB-SAL ($p < 0.05$).
[#] OB-SAL *vs.* OB-OVA ($p < 0.05$).

Table 4
Semi-quantitative analysis of electron microscopy.

	C		OB	
	SAL	OVA	SAL	OVA
Epithelial detachment	0 (0–0)	2 (2–2.25)[*]	0 (0–0)	4 (3–4)[**,#]
Eosinophil infiltration	0 (0–0)	2 (2–2.25)[*]	0 (0–1)	3 (3–3.25)[**,#]
Neutrophil infiltration	0 (0–0)	2 (1–2.25)[*]	1(0.75–1)[†]	3 (3–4)[**,#]
Disorganization of ciliated cells	0 (0–0)	2 (2–2.25)[*]	0 (0–0)	3 (2.75–4)[#]
Subephitelial fibrosis	0 (0–0)	2 (2–2.25)[*]	1 (0.75–1)[†]	3 (3–4)[**,#]
Elastic fiber fragmentation	0 (0–0)	2 (2–3)[*]	0 (0–0)	4 (3–4)[**,#]
Smooth muscle hypertrophy	0 (0–0)	3 (2–3)[*]	0 (0–0)	3 (2.75–3.25)[#]
Myofibroblasts hyperplasia	0 (0–0)	3 (2–3)[*]	0 (0–0)	3 (3–4)[#]
Mucous cells hyperplasia	0 (0–0)	2 (2–2.25)[*]	0 (0–0)	3 (3–4)[**,#]

Values are median (25th to 75th percentile) of five mice in each group. C: mice fed with a standard chow diet, OB: animals that received isocaloric high-fat diet. SAL: mice sensitized and challenged with saline, OVA: mice sensitized and challenged with ovalbumin.
[*] C-SAL *vs.* C-OVA ($p < 0.05$).
[**] C-OVA *vs.* OB-OVA ($p < 0.05$).
[†] C-SAL *vs.* OB-SAL ($p < 0.05$).
[#] OB-SAL *vs.* OB-OVA ($p < 0.05$).

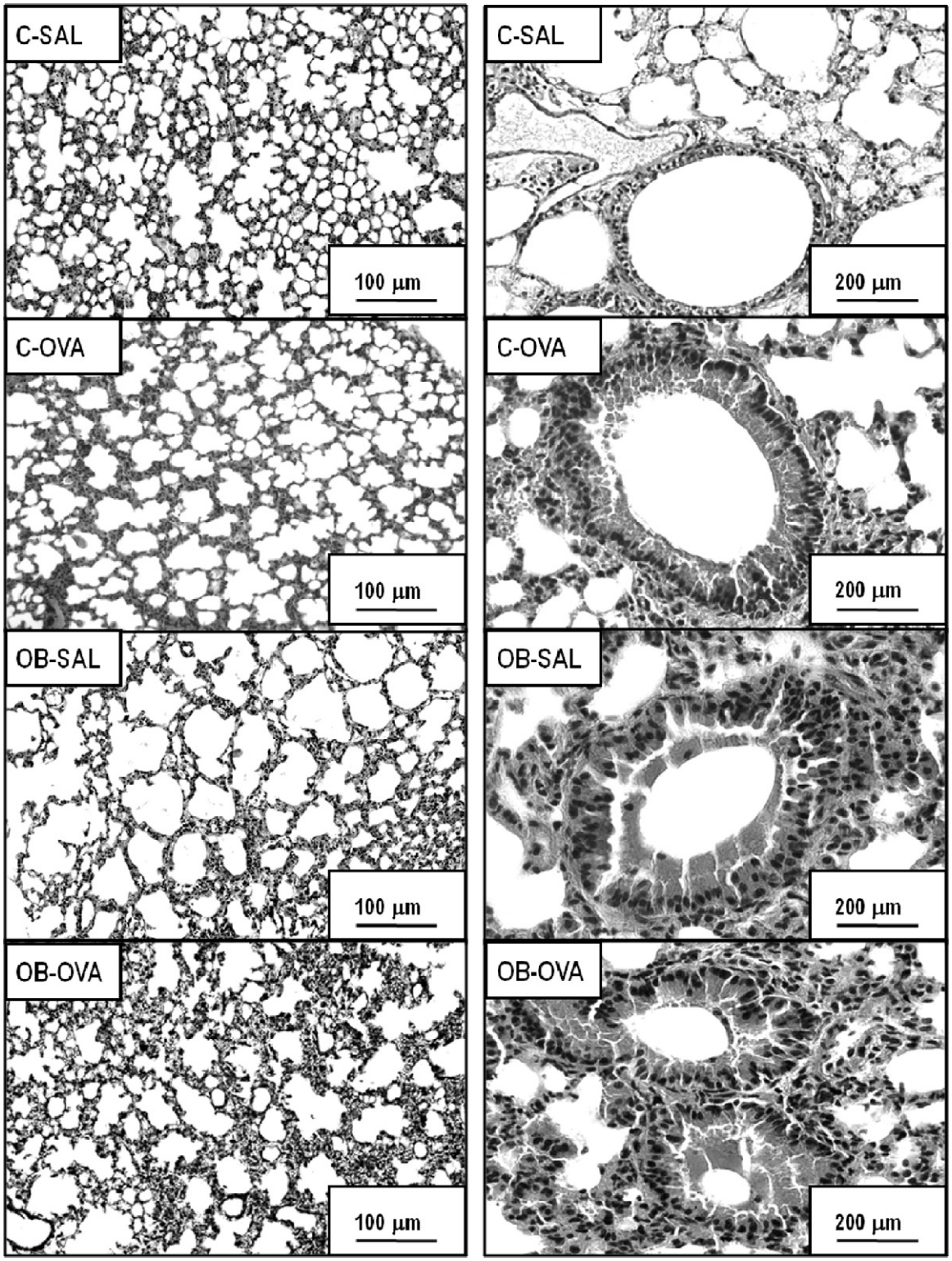

Fig. 1. Representative photomicrographs of lung parenchyma (left) and airway (right) stained with hematoxylin–eosin. C: mice fed with a standard chow diet, OB: animals receiving isocaloric high-fat diet. SAL: mice sensitized and challenged with saline, OVA: mice sensitized and challenged with ovalbumin. Photomicrographs were taken at an original magnification of 200× (lung parenchyma) and 400× (airway). Scale bars = 100 μm.

asthma. Collagen fiber and α-smooth muscle actin contents and ultrastructural airway changes (such as subepithelial fibrosis, elastic fiber fragmentation, and mucous cell hyperplasia) were also more prominent in OB-OVA. Furthermore, obesity yielded an additional increase in total and differential cell counts in the BALF of OVA animals.

Instead of using genetically obese mice, we induced obesity with a high fat diet supplemented with lard and soybean oil. This was done because genetically modified animals present a smaller lung size (Shore et al., 2003; Shore, 2007) associated with reduced lung volumes and decreased lung mass, which may affect the remodeling process. The literature reports induction of obesity by a high

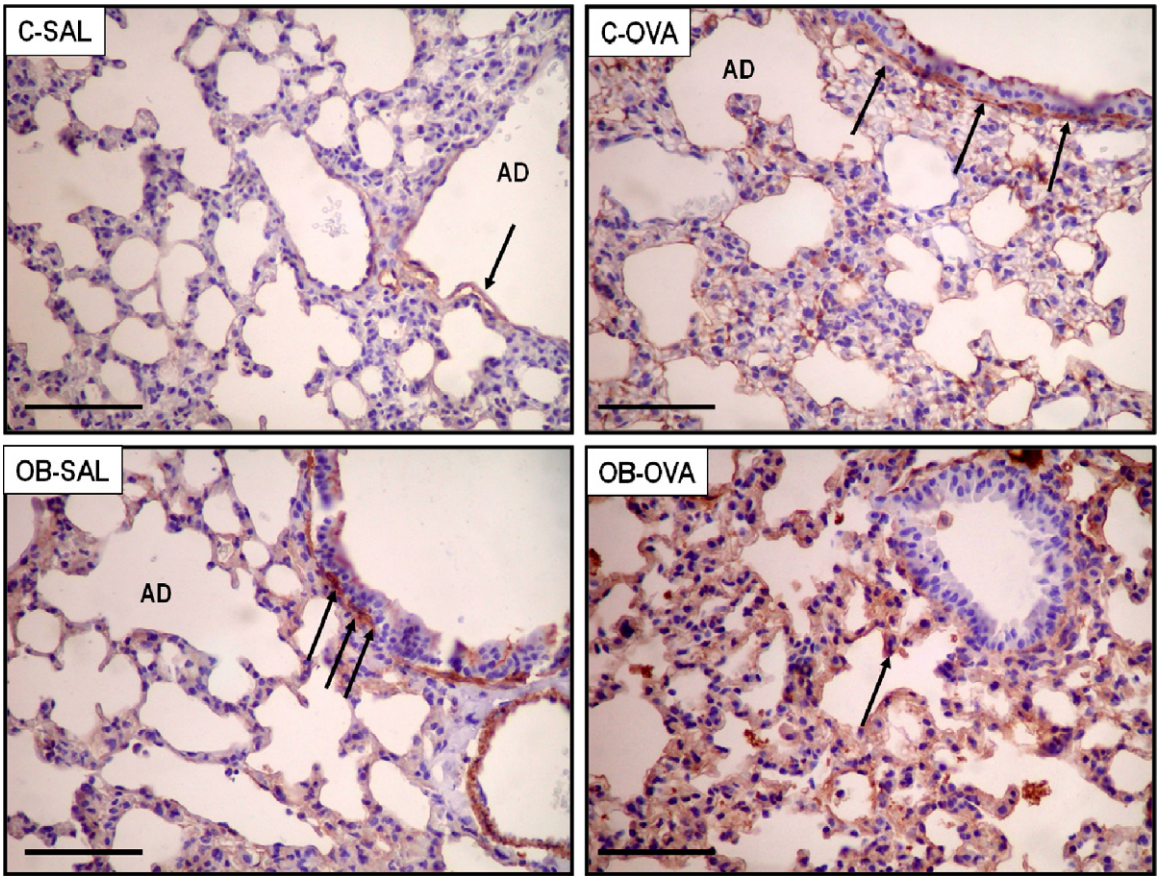

Fig. 2. Immunohistochemical staining for smooth-muscle-specific actin. C: mice fed with a standard chow diet, OB: animals receiving isocaloric high-fat diet. SAL: mice sensitized and challenged with saline, OVA: mice sensitized and challenged with ovalbumin. AD: alveolar duct. Note positive brown-reddish staining for α-actin in bronchiole and alveoli. Scale bars = 400 μm.

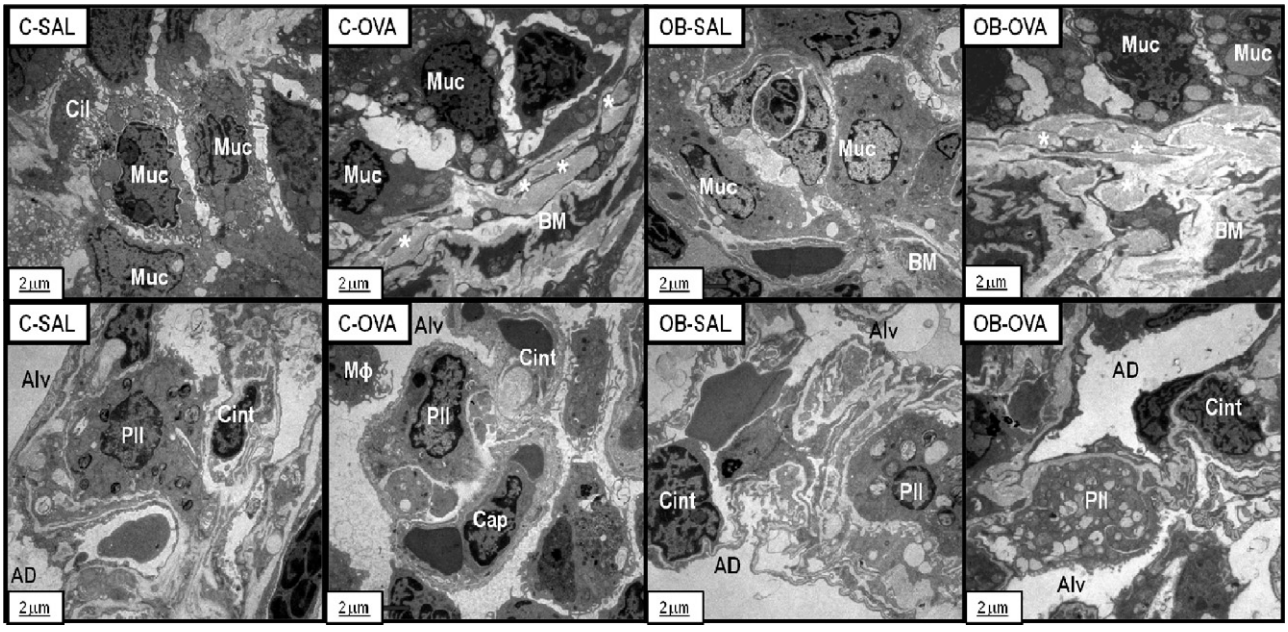

Fig. 3. Electron microscopy of airway (upper panels) and lung parenchyma (lower panels). Mucous cells (Muc), ciliate cells (Cil), basal membrane (BM), interstitial cell (Cint), macrophage (Mϕ), capillary (Cap), alveolar duct (AD), and alveolar space (Alv). Asterisk: collagen fiber. Note in OVA group epithelial damage in the terminal bronchioles with mucous cell hypertrophy, thickness of basal membrane, mainly in OB mice. Furthermore, note the integrity of type II alveolar epithelial cell (PII) in all groups.

Table 5
Bronchoalveolar lavage fluid cellularity.

	C		OB	
	SAL	OVA	SAL	OVA
Leukocytes ($\times 10^5$/BAL)	1.18 ± 0.19	4.04 ± 0.94*	1.82 ± 0.16†	9.75 ± 3.07**,#
Monocytes ($\times 10^5$/BAL)	1.09 ± 0.11	1.80 ± 0.02*	1.59 ± 0.19†	5.23 ± 0.43**,#
Eosinophils ($\times 10^5$/BAL)	0.02 ± 0.02	1.44 ± 0.01*	0.03 ± 0.01	2.65 ± 0.65**,#
Neutrophils ($\times 10^5$/BAL)	0.07 ± 0.01	0.80 ± 0.08*	0.20 ± 0.01†	1.87 ± 0.47**,#

Total and differential cellularity in bronchoalveolar lavage fluid (BALF). Values are mean (±SEM) of 7 animals in each group. C: mice fed with a standard chow diet, OB: animals that received isocaloric high-fat diet. SAL: mice sensitized and challenged with saline, OVA: mice sensitized and challenged with ovalbumin.

* C-SAL *vs.* C-OVA ($p < 0.05$).
** C-OVA *vs.* OB-OVA ($p < 0.05$).
† C-SAL *vs.* OB-SAL ($p < 0.05$).
# OB-SAL *vs.* OB-OVA ($p < 0.05$).

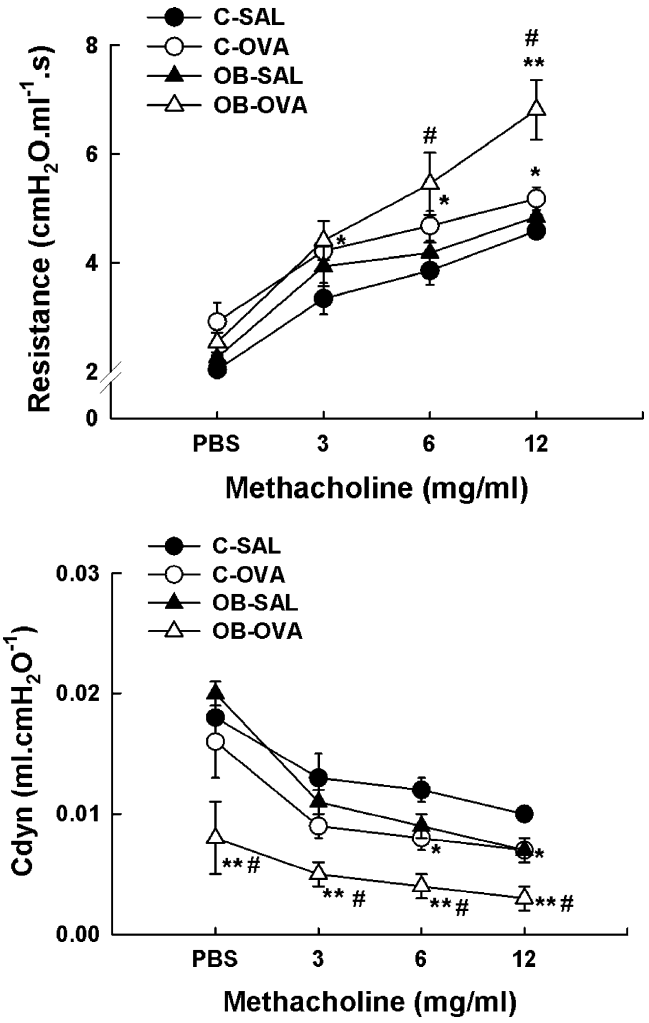

Fig. 4. Airway resistance and dynamic compliance after increasing methacholine doses. Values are means (±SEM) of 5 animals in each group. C: mice fed with a standard chow diet, OB: animals receiving isocaloric high-fat diet. SAL: mice sensitized and challenged with saline, OVA: mice sensitized and challenged with ovalbumin. Airway resistance was measured in response to increasing doses of methacholine. *C-SAL *vs.* C-OVA ($p < 0.05$), **C-OVA *vs.* OB-OVA ($p < 0.05$), #OB-SAL *vs.* OB-OVA ($p < 0.05$).

fat diet in C57BL/6 mice (Johnston et al., 2007), but pilot studies have demonstrated that the animals' acceptance of the diet reduced significantly after the second week. A similar behavior was also observed in BALB/c mice. In this line, some mouse strains are responsive to dietary obesity when fed a diet containing moderate levels of fat, while other strains are not responsive and do not become obese when fed the same diet (West et al., 1992). Furthermore, lung parenchyma remodeled differently and presented distinct tissue mechanics depending on mouse strain (Antunes et al., 2009). In the current study, A/J mice were used, and after 12 weeks the total body mass was substantially greater (50%) in animals receiving the high fat diet than in those receiving the standard diet. Similar to genetically obese mice, the increase in the total body mass of A/J mice with a high fat diet is almost entirely due to an increase in fat mass (Black et al., 1998).

The present asthma protocol was able to reproduce some aspects of chronic human asthma, such as airway hyperresponsiveness, BALF eosinophilia, smooth muscle hypertrophy, basement membrane thickness, and mucous gland hyperplasia (Xisto et al., 2005).

Obesity yielded larger chest wall circumferences, which resulted in lower tidal volume, alveolar collapse, and a reduction in the diameter of airways. However, in the presence of obesity, asthma is not simply a mechanical phenomenon. In this line, Shore and colleagues have shown that obese mice have increased airway hyperresponsiveness independent of lung volume (Shore, 2007), possibly associated with augmentation of the inflammatory process (Ding et al., 1987; Fredberg et al., 1999). In the present study, obesity led to an increase in the inflammatory process observed in BALF and lung histology, especially after the induction of asthma. However, we cannot rule out a role of the remodeling process in increasing airway hyperresponsiveness. The greater extracellular matrix remodeling in obese mice with asthma was characterized by increased collagen deposition, α-smooth muscle actin content, and ultrastructural degeneration of airways (epithelial detachment, subepithelial fibrosis, elastic fiber fragmentation, smooth muscle hypertrophy, myofibroblast hyperplasia, and mucous cell hyperplasia). The impact of obesity on the remodeling process may result from chronic repetitive injury to the airway wall caused by inflammation even though inflammation is not necessarily related to remodeling in a quantitative manner (Locke et al., 2007; Abreu et al., 2010; Antunes et al., 2010). In this context, increased IL-4 and IL-5 may play a role in the regulation of collagen synthesis by stimulating transforming growth factors (TGF-β) and increasing the expression of type I collagen through activation of transcription factors (Wen et al., 2003; Tanaka et al., 2004). Furthermore, VEGF may also cause a marked increase in inflammation, followed by an increase in mononuclear cells, eosinophils, and neutrophils (Homer and Elias, 2005).

To the best of our knowledge, no other study has analyzed an experimental mouse model of obesity and chronic allergic asthma evaluating not only airway inflammatory and remodeling processes, but also the interaction between them. Nevertheless, our study presents limitations. The impact of obesity in asthma is more pronounced in females than in males. In the present study, male mice were used, limiting the elucidation of a gender effect. Secondly, we were unable to gather data on leptin and adiponectin levels due to technical problems in the A/J mice. The levels of both

hormones are increased in obesity and may influence asthma development (Shore et al., 2005; Medoff et al., 2009). Third, inflammatory and fibrogenic mediators were not measured, due to the difficulty in obtaining a consistent pattern in this strain of mouse, preventing a more detailed understanding of remodeling mechanisms. Finally, the Buxco Pulmonary Mechanics Processing System is unable to analyse proximal and distal airways separately. However, even though lung histology was analyzed mainly in distal airways, it was able to reveal an impact of obesity on airway hyperresponsiveness and dynamic compliance.

In conclusion, in the present experimental model of chronic allergic asthma, obesity induced greater lung inflammation and remodeling, which were associated with increased airway responsiveness to methacholine. Our experimental study indicates that obesity influences asthma severity by contributing to both the inflammatory and remodeling processes.

Acknowledgements

The authors would like to express their gratitude to Mr. Andre Benedito da Silva for animal care, Mrs. Thaiana Borges and for her skilful technical assistance during the experiments, Mrs. Ana Lucia Neves da Silva for her help with microscopy, and Mrs. Moira Elizabeth Schöttler and Claudia Buchweitz for their assistance in editing the manuscript.

This study was supported by Centers of Excellence Program (PRONEXFAPERJ), Brazilian Council for Scientific and Technological Development (CNPq), Rio de Janeiro State Research Supporting Foundation (FAPERJ), Coordination for the Improvement of Higher Education Personnel (CAPES), and São Paulo State Research Supporting Foundation (FAPESP).

References

Abreu, S.C., Antunes, M.A., Maron-Gutierrez, T., Cruz, F.F., Carmo, L.G., Ornellas, D.S., Junior, H.C., Absaber, A.M., Parra, E.R., Capelozzi, V.L., Morales, M.M., Rocco, P.R., 2010. Effects of bone marrow-derived mononuclear cells on airway and lung parenchyma remodeling in a murine model of chronic allergic inflammation. Respir. Physiol. Neurobiol. 175, 153–163.

Antunes, M.A., Abreu, S.C., Damaceno-Rodrigues, N.R., Parra, E.R., Capelozzi, V.L., Pinart, M., Romero, P.V., Silva, P.M., Martins, M.A., Rocco, P.R., 2009. Different strains of mice present distinct lung tissue mechanics and extracellular matrix composition in a model of chronic allergic asthma. Respir. Physiol. Neurobiol. 165, 202–207.

Antunes, M.A., Abreu, S.C., Silva, A.L., Parra-Cuentas, E.R., Ab'Saber, A.M., Capelozzi, V.L., Ferreira, T.P., Martins, M.A., Silva, P.M., Rocco, P.R., 2010. Sex-specific lung remodeling and inflammation changes in experimental allergic asthma. J. Appl. Physiol. 109, 855–863.

Bateman, E.D., Hurd, S.S., Barnes, P.J., Bousquet, J., Drazen, J.M., FitzGerald, M., Gibson, P., Ohta, K., O'Byrne, P., Pedersen, S.E., Pizzichini, E., Sullivan, S.D., Wenzel, S.E., Zar, H.J., 2008. Global strategy for asthma management and prevention: GINA executive summary. Eur. Respir. J. 31, 143–178.

Black, B.L., Croom, J., Eisen, E.J., Petro, A.E., Edwards, C.L., Surwit, R.S., 1998. Differential effects of fat and sucrose on body composition in A/J and C57BL/6 mice. Metabolism 47, 1354–1359.

Calixto, M.C., Lintomen, L., Schenka, A., Saad, M.J., Zanesco, A., Antunes, E., 2010. Obesity enhances eosinophilic inflammation in a murine model of allergic asthma. Br. J. Pharmacol. 159, 617–625.

Davies, D.E., Wicks, J., Powell, R.M., Puddicombe, S.M., Holgate, S.T., 2003. Airway remodeling in asthma: new insights. J. Allergy Clin. Immunol. 111, 215–225, quiz 226.

Ding, D.J., Martin, J.G., Macklem, P.T., 1987. Effects of lung volume on maximal methacholine-induced bronchoconstriction in normal humans. J. Appl. Physiol. 62, 1324–1330.

Dixon, A.E., Holguin, F., Sood, A., Salome, C.M., Pratley, R.E., Beuther, D.A., Celedon, J.C., Shore, S.A., 2010. An official American Thoracic Society Workshop report: obesity and asthma. Proc. Am. Thorac. Soc. 7, 325–335.

Dolhnikoff, M., Morin, J., Ludwig, M.S., 1998. Human lung parenchyma responds to contractile stimulation. Am. J. Respir. Crit. Care Med. 158, 1607–1612.

Elias, J.A., Zhu, Z., Chupp, G., Homer, R.J., 1999. Airway remodeling in asthma. J. Clin. Invest. 104, 1001–1006.

Fredberg, J.J., Inouye, D.S., Mijailovich, S.M., Butler, J.P., 1999. Perturbed equilibrium of myosin binding in airway smooth muscle and its implications in bronchospasm. Am. J. Respir. Crit. Care Med. 159, 959–967.

Fullmer, H.M., Sheetz, J.H., Narkates, A.J., 1974. Oxytalan connective tissue fibers: a review. J. Oral Pathol. 3, 291–316.

Homer, R.J., Elias, J.A., 2005. Airway remodeling in asthma: therapeutic implications of mechanisms. Physiology (Bethesda) 20, 28–35.

Hsia, C.C., Hyde, D.M., Ochs, M., Weibel, E.R., 2010. An official research policy statement of the American Thoracic Society/European Respiratory Society: standards for quantitative assessment of lung structure. Am. J. Respir. Crit. Care Med. 181, 394–418.

Jeffery, P.K., Godfrey, R.W., Adelroth, E., Nelson, F., Rogers, A., Johansson, S.A., 1992. Effects of treatment on airway inflammation and thickening of basement membrane reticular collagen in asthma. A quantitative light and electron microscopic study. Am. Rev. Respir. Dis. 145, 890–899.

Johnston, R.A., Zhu, M., Rivera-Sanchez, Y.M., Lu, F.L., Theman, T.A., Flynt, L., Shore, S.A., 2007. Allergic airway responses in obese mice. Am. J. Respir. Crit. Care Med. 176, 650–658.

Locke, N.R., Royce, S.G., Wainewright, J.S., Samuel, C.S., Tang, M.L., 2007. Comparison of airway remodeling in acute, subacute, and chronic models of allergic airways disease. Am. J. Respir. Cell Mol. Biol. 36, 625–632.

Maranhão, E., Barboza, A.P., Ciminelli, P.B., Alcantara, B.J., Berti, M., Oliveira-Neto, J., Capelozzi, V.L., Zin, W.A., Rocco, P.R., 2000. Temporal evolution of pneumothorax: respiratory mechanical and histopathological study. Respir. Physiol. 119, 41–50.

Medoff, B.D., Okamoto, Y., Leyton, P., Weng, M., Sandall, B.P., Raher, M.J., Kihara, S., Bloch, K.D., Libby, P., Luster, A.D., 2009. Adiponectin deficiency increases allergic airway inflammation and pulmonary vascular remodeling. Am. J. Respir. Cell Mol. Biol. 41, 397–406.

Menezes, S.L., Bozza, P.T., Neto, H.C., Laranjeira, A.P., Negri, E.M., Capelozzi, V.L., Zin, W.A., Rocco, P.R., 2005. Pulmonary and extrapulmonary acute lung injury: inflammatory and ultrastructural analyses. J. Appl. Physiol. 98, 1777–1783.

Misso, N.L., Petrovic, N., Grove, C., Celenza, A., Brooks-Wildhaber, J., Thompson, P.J., 2008. Plasma phospholipase A2 activity in patients with asthma: association with body mass index and cholesterol concentration. Thorax 63, 21–26.

Montes, G.S., 1996. Structural biology of the fibres of the collagenous and elastic systems. Cell Biol. Int. 20, 15–27.

Santos, F.B., Nagato, L.K., Boechem, N.M., Negri, E.M., Guimaraes, A., Capelozzi, V.L., Faffe, D.S., Zin, W.A., Rocco, P.R., 2006. Time course of lung parenchyma remodeling in pulmonary and extrapulmonary acute lung injury. J. Appl. Physiol. 100, 98–106.

Shore, S.A., 2007. Obesity and asthma: lessons from animal models. J. Appl. Physiol. 102, 516–528.

Shore, S.A., Fredberg, J.J., 2005. Obesity, smooth muscle, and airway hyperresponsiveness. J. Allergy Clin. Immunol. 115, 925–927.

Shore, S.A., Rivera-Sanchez, Y.M., Schwartzman, I.N., Johnston, R.A., 2003. Responses to ozone are increased in obese mice. J. Appl. Physiol. 95, 938–945.

Shore, S.A., Schwartzman, I.N., Mellema, M.S., Flynt, L., Imrich, A., Johnston, R.A., 2005. Effect of leptin on allergic airway responses in mice. J. Allergy Clin. Immunol. 115, 103–109.

Shore, S.A., Terry, R.D., Flynt, L., Xu, A., Hug, C., 2006. Adiponectin attenuates allergen-induced airway inflammation and hyperresponsiveness in mice. J. Allergy Clin. Immunol. 118, 389–395.

Silva, P.L., Passaro, C.P., Cagido, V.R., Bozza, M., Dolhnikoff, M., Negri, E.M., Morales, M.M., Capelozzi, V.L., Zin, W.A., Rocco, P.R., 2008. Impact of lung remodelling on respiratory mechanics in a model of severe allergic inflammation. Respir. Physiol. Neurobiol. 160, 239–248.

Tanaka, H., Komai, M., Nagao, K., Ishizaki, M., Kajiwara, D., Takatsu, K., Delespesse, G., Nagai, H., 2004. Role of interleukin-5 and eosinophils in allergen-induced airway remodeling in mice. Am. J. Respir. Cell Mol. Biol. 31, 62–68.

Weibel, E.R., 1990. Morphometry: stereological theory and practical methods. In: J, G. (Ed.), Models of Lung Disease-Microscopy and Structural Methods. Marcel Dekker, New York, pp. 199–247.

Wen, F.Q., Liu, X.D., Terasaki, Y., Fang, Q.H., Kobayashi, T., Abe, S., Rennard, S.I., 2003. Interferon-gamma reduces interleukin-4- and interleukin-13-augmented transforming growth factor-beta2 production in human bronchial epithelial cells by targeting Smads. Chest 123, 372S–373S.

West, D.B., Boozer, C.N., Moody, D.L., Atkinson, R.L., 1992. Dietary obesity in nine inbred mouse strains. Am. J. Physiol. 262, R1025–R1032.

Xisto, D.G., Farias, L.L., Ferreira, H.C., Picanco, M.R., Amitrano, D., Lapa, E.S.J.R., Negri, E.M., Mauad, T., Carnielli, D., Silva, L.F., Capelozzi, V.L., Faffe, D.S., Zin, W.A., Rocco, P.R., 2005. Lung parenchyma remodeling in a murine model of chronic allergic inflammation. Am. J. Respir. Crit. Care Med. 171, 829–837.

Zin, W.A., Martins, M.A., Silva, P.R., Sakae, R.S., Carvalho, A.L., Saldiva, P.H., 1989. Effects of abdominal opening on respiratory system mechanics in ventilated rats. J. Appl. Physiol. 66, 2496–2501.